

3D Analysis of the incident diffuse irradiance on the building's surfaces in an urban environment

Stoyanka M. Ivanova ^{1*}

¹ *University of Architecture, Civil Engineering and Geodesy, Sofia, Bulgaria*

**Corresponding author: telephone: +359 89 9966332, e-mail: solaris@online.bg*

Abstract

The design of a future building with very high energy efficiency demands from the architect to study the available solar resources in this urban environment. The purpose of the presented methodology is to study the variations in all components of the incident solar radiation daily, monthly and seasonally for all building facades. This is realized in the computer program 3D-SOLARIA. In the focus of the paper is the estimation of the background component of the incident diffuse solar irradiation on a building facade under orthogonally obstructed sky, using anisotropic sky view factors.

Keywords

Solar irradiance, Anisotropic sky model, Anisotropic view factors, Partially obstructed sky, Urban environment

1 Introduction

The European directive on the energy performance of the buildings prescribes very high energy efficiency of the new buildings. For this purpose the architect has to know the solar resources for the future building in the early design stage, when he shapes his idea. Daily, monthly and seasonal variations in the incident solar irradiation on the all building surfaces are important. Their analysis is a difficult task in an urban environment because of the presence of many obstructing objects – buildings, installations, vegetation, etc. The seasonal analysis could help the architect to differentiate the opposite needs of solar energy in the winter and summer (more solar energy in the winter and less solar energy in the summer).

The solving methods vary from very simple ones (with angular criteria and angular zones) to very complex, which divide the sky into hundreds of patches. Two examples are the programs SUNtool – CITYSIM [1] and Solar Radiation Technology to Revit. They divide every building surface into small fragments and study the visibility to their centers of each sky patch in relation to each potentially obstructing object. This solving method needs a lot of computer time. Its advantage is that it could work with objects in any shape and in any position.

2 Methodology

Most objects in an urban environment have orthogonal surfaces, which are perpendicular or parallel to each other. This allowed us to develop an analytical approach [2] to both receiving and obstructing rectangular building surfaces, without the usage of hundreds of sky patches. The estimation of the incident diffuse solar irradiation and especially its background component is in the focus of this paper.

2.1 Anisotropic radiance model

Our approach needs a suitable anisotropic radiance model to be able to predict the radiance in any point of the sky in any time, and to be applied for overcast, non-overcast and “real” sky. An irradiance model has to predict correctly the irradiance values on a sloped surface. The anisotropic model of Muneer [3] is used as a base model for the presented approach, because it is one of the most used anisotropic irradiance models and has some features of a radiance model with the usage of the equation of Moon & Spencer about the luminance distribution under overcast sky $L_{\theta}=L_z(1+b.\cos\theta)/(1+b)$. Steven and Unsworth and later Usher and Muneer integrated this equation to obtain the ratio between the irradiance on a sloped surface $I_{D\beta}$ and the horizontal diffuse irradiance I_{DH} under overcast sky – Eq. (1):

$$T = \frac{I_{D\beta}}{I_{DH}} = \cos^2\left(\frac{\beta}{2}\right) + \frac{2b}{\pi(3+2b)} \left[\sin(\beta) - \beta.\cos(\beta) - \pi.\sin^2\left(\frac{\beta}{2}\right) \right] \quad (1)$$

Muneer's model estimates the diffuse irradiance on a sloped sunlit surface under non-overcast sky as follows – Eq. (2):

$$I_{D\beta} = I_{DH} [T(1-F) + F.r_B] \quad (2)$$

where F is the ratio between the beam and the extraterrestrial horizontal irradiances, T is calculated as a function of the radiance distribution index b and slope angle β in Eq. (1), and $r_B = \cos(i)/\sin(h)$ is the beam conversion factor. The circumsolar brightening is simplified as concentrated at the position of the sun. The interdependence between b and F is visible in the Eq. (3) by Muneer [3] with parameters' values $a_1 = 0.00333$; $a_2 = -0.415$; $a_3 = -0.6987$ for northern Europe and $a_1 = 0.00263$; $a_2 = -0.712$; $a_3 = -0.6883$ for southern Europe.

$$\frac{2b}{\pi(3+2b)} = a_1 + a_2F + a_3F^2 \quad (3)$$

Muneer estimates the diffuse irradiance on a sloped shaded surface under non-overcast sky with the same equation $I_{D\beta} = I_{DH}T$ as for a sloped surface under an overcast sky. There T depends on $b=5.73$, even if this means the background radiance at the horizon is calculated of less value than the background zenith radiance, which obviously is not true for a clear sky. This separately treating of sunlit and shaded surfaces with different values of b leads to internal contradiction. If the receiving surface is horizontal or with a small slope angle, the irradiance coming from the southern and northern halves of the sky has to be modeled with “sunlit” (negative) values of b – Eq. (3). If the receiving surface is shaded, the same areas in the northern half of the sky dome has to be modeled with “shaded” (positive) value $b=5.73$.

Most other models (Hay and Davies; Hay and McKay; Ma-Iqbal) accept that the background diffuse component is the same for sunlit and for shaded surfaces under a non-overcast sky and use F (or other sky clarity index) as a value, which mixes the background and the circumsolar components. Such approach helps to avoid the mentioned internal contradiction. If we apply this approach to Muneer's model we can distinguish as independent both components $I_{BD\beta}$ and $I_{CD\beta}$ of the diffuse irradiance on a sloped surface as follows:

$$I_{BD\beta} = I_{DH}(1-F) \left\{ \cos^2\left(\frac{\beta}{2}\right) + \frac{2b}{\pi(3+2b)} \left[\sin(\beta) - \beta.\cos(\beta) - \pi.\sin^2\left(\frac{\beta}{2}\right) \right] \right\} \quad (4)$$

$$I_{CD\beta} = I_{DH}F.r_B \quad (5)$$

For a horizontal surface ($T=1$ and $r_B=1$) under an unobstructed sky the background and the circumsolar components of the diffuse irradiance are estimated as follows:

$$I_{BDH} = I_{DH}(1-F) \quad (6)$$

$$I_{CDH} = I_{DH}F \quad (7)$$

For northern Europe and a value $F=0.5625$ the estimated ratio of the vertical diffuse irradiance to the horizontal diffuse irradiance is 0.331, which is very close to the measured data for European sites. This ratio varies daily and hourly as it is a function of the ratio F between the beam and the extraterrestrial horizontal irradiances. Anyway sometimes the calculated too low values of b (too close to -1) indicate an overestimated horizon brightening and a need of a recalibration of the model.

2.2 Basic anisotropic sky view factors

In order to predict the incident background diffuse solar radiation on a building, we need to estimate it for any of its external surfaces. When we know the horizontal diffuse irradiance, we can find its background component with Eq. (6). Later our task is to find the ratio between the background diffuse irradiance from a partially obstructed anisotropic sky onto a building's surface and the background horizontal diffuse irradiance from an unobstructed anisotropic sky. In [2] we named this ratio **anisotropic background sky view factor** (horizontal, vertical and sloped). More detailed information how to estimate the anisotropic vertical factor (AVF) from the visible sky area to a point on a vertical surface (fragment) is given there. The basic considered sky sectors are displayed on Figure 1.

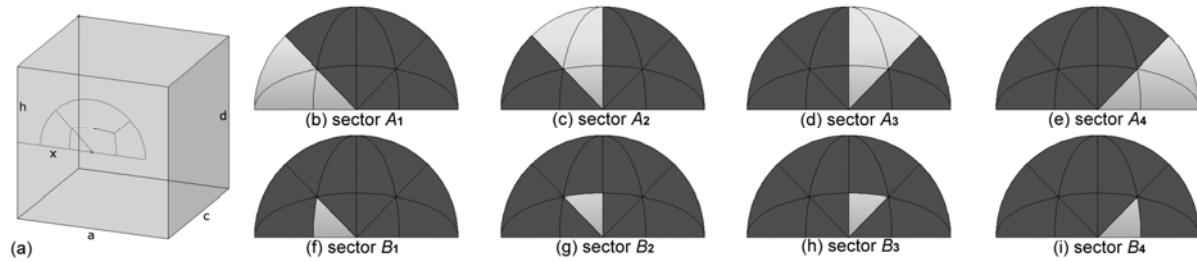


Fig. 1 Basic considered sky sectors, displayed on a rectangular cuboid with dimensions $a \times c \times d$, with a stereographic projection onto a point on a cuboid's vertical wall. The point is at distance x from the left vertical edge and at distance h from the top horizontal edge of the studied vertical wall. The projections of the other lines of the cuboid's edges delimit the basic considered sky sectors: circular sectors A_1, A_2, A_3, A_4 ; elliptic sectors B_1, B_2, B_3, B_4

2.3 Derivative anisotropic sky view factors

With combinations of sums and differences of the AVF of the mentioned basic sectors we can estimate the value of the AVF of each visible part of sky in case it is obstructed by one or more orthogonally orientated horizontal or vertical surfaces (Figure 2).

The stereographic projections on Figure 2a to 2e look like interiors, but the estimated AVF for the sky areas could be subtracted from the maximum possible value of an AVF for a vertical surface: $(3\pi+4b)/[2\pi(3+2b)]$. This way we receive the resulting value of AVF of the visible sky areas toward an exterior wall (façade) as in Figure 2f, 2g, etc.

The resulting Eqs. (8) to (10) for AVF of the three most widely used combined projections: A_1-B_1 (Figure 2a), A_2-B_2 (Figure 2b), B_1+B_2 (Figure 2c) are listed below:

$$AVF_{A_1-B_1 \rightarrow point} = \frac{3}{3+2b} \cdot \frac{1}{2\pi} \left(\arctg \frac{h}{x} - \frac{x}{\sqrt{x^2+c^2}} \arctg \frac{h}{\sqrt{x^2+c^2}} \right) + \frac{2b}{3+2b} \cdot \frac{1}{2\pi} \left(1 - \frac{x}{\sqrt{x^2+h^2}} - \frac{x}{\sqrt{x^2+c^2}} + \frac{x}{\sqrt{x^2+c^2+h^2}} \right) \quad (8)$$

$$AVF_{A_2-B_2 \rightarrow point} = \frac{3}{3+2b} \cdot \frac{1}{2\pi} \left(\arctg \frac{x}{h} - \frac{h}{\sqrt{c^2+h^2}} \arctg \frac{x}{\sqrt{c^2+h^2}} \right) + \frac{2b}{3+2b} \cdot \frac{1}{2\pi} \left(\frac{x}{\sqrt{x^2+h^2}} - \frac{xh^2}{(c^2+h^2)\sqrt{x^2+c^2+h^2}} \right) \quad (9)$$

$$AVF_{B_1+B_2 \rightarrow point} = \frac{3}{3+2b} \cdot \frac{1}{2\pi} \left(\frac{x}{\sqrt{x^2+c^2}} \arctg \frac{h}{\sqrt{x^2+c^2}} + \frac{h}{\sqrt{c^2+h^2}} \arctg \frac{x}{\sqrt{c^2+h^2}} \right) + \frac{2b}{3+2b} \cdot \frac{1}{2\pi} \left(\frac{x}{\sqrt{x^2+c^2}} - \frac{x}{\sqrt{x^2+c^2+h^2}} + \frac{xh^2}{(c^2+h^2)\sqrt{x^2+c^2+h^2}} \right) \quad (10)$$

These three equations include two parts. The isotropic part P_i multiplied by $3/(3+2b)$ is the isotropic view factor for the specific sector. The anisotropic part P_a multiplied by $2b/(3+2b)$ is an anisotropic correction of the isotropic view factor. Both isotropic and anisotropic parts depend only on geometric data. They can be calculated once for each considered point and then to be used in combination with the varying value of b for different time periods.

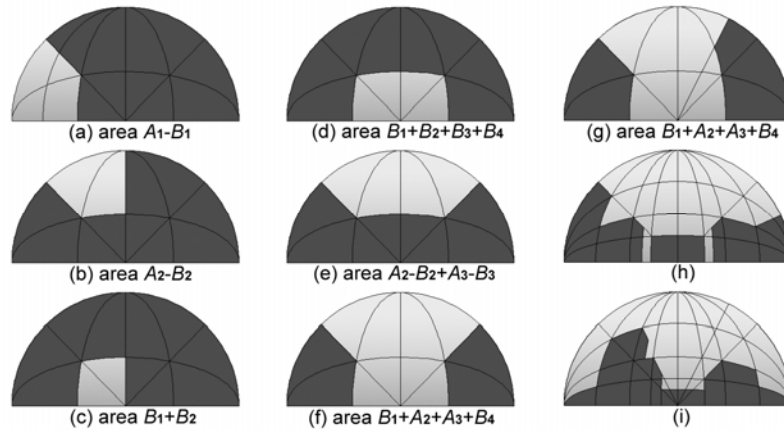


Fig. 2 Combined projections: (a) area A_1-B_1 ; (b) area A_2-B_2 ; (c) area B_1+B_2 ; (d) area $(B_1+B_2)+(B_3+B_4)$; (e) area $(A_2-B_2)+(A_3-B_3)$; (f) area $(B_1+A_2)+(A_3+B_4)$; (g), (h), (i) more complex projections

3 Results

Using described methodology and solar data from PVGIS [4], we developed a computer program **3D-SOLARIA** to estimate, display and study all components of the solar irradiance and solar irradiation for different time periods (days, months, seasons) on the rectangular fragments of all vertical walls of a considered building.

The order of tasks to estimate the AVF of a fragment of a vertical wall is as follows:

- (a) Analysis of the visibility of all other vertical walls of the considered building and other obstructing buildings.
- (b) Estimation of AVF of all partially and completely visible vertical walls. These estimated values are summarized in the value $AVF_{visible_walls}$.

(c) Estimation of AVF of all hidden parts of partially visible vertical walls. These estimated values are summarized in the value $AVF_{invisible_parts}$.

(d) The value of $AVF_{visible_sky}$ from the visible part of the sky is estimated as follows:

$$AVF_{visible_sky} = \frac{3}{3+2b} \left(\frac{1}{2} - \sum_{k=1}^{N_{visible_walls}} P_{i_k} + \sum_{j=1}^{N_{invisible_parts}} P_{i_j} \right) + \frac{2b}{3+2b} \left(\frac{1}{\pi} - \sum_{k=1}^{N_{visible_walls}} P_{a_k} + \sum_{j=1}^{N_{invisible_parts}} P_{a_j} \right) \quad (11)$$

The four sums in Eq. (11) have to be estimated once for each fragment of the considered wall. For each varying value of b we estimate $AVF_{visible_sky}$ and use it to calculate the background diffuse irradiance $I_{bd_fragment}$ in the center point of the vertical fragment as follows:

$$I_{bd_fragment} = AVF_{visible_sky} I_{BDH} \quad (12)$$

To the estimated value then we add the values of estimated circumsolar component of the diffuse irradiance, the beam and reflected irradiance.

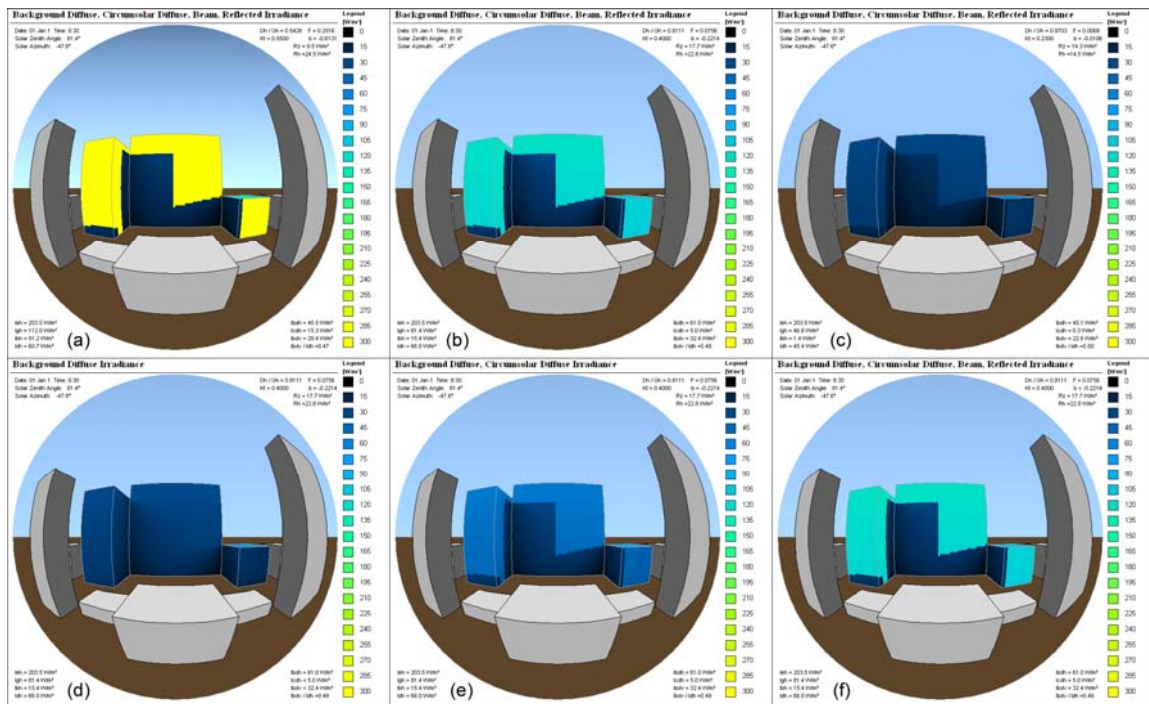


Fig. 3 Exemplary images, generated in 3D-SOLARIA Irradiance Mode for January 1st, 8:30 in Sofia: (a) solar irradiance – $D/G=0.54$, $K_t=0.55$; (b) solar irradiance – $D/G=0.81$, $K_t=0.4$; (c) solar irradiance – $D/G=0.97$, $K_t=0.23$; (d) background diffuse irradiance – $D/G=0.81$; (e) diffuse irradiance – $D/G=0.81$; (f) diffuse, beam and reflected irradiance – $D/G=0.81$

The program has two modes. In Irradiance mode it calculates the instantaneous density of the solar radiation [W/m^2] incident on the fragments of all considered walls in different time moments – Figure 3. Different kinds of skies are considered, using the Muneer's Eq. (13) from [3]:

$$D/G = 1.006 - 0.317K_t + 3.1241K_t^2 - 12.7616K_t^3 + 9.7166K_t^4 \quad (13)$$

In Irradiation mode the program calculates and displays the average daily irradiation [Wh/m^2] on the considered fragments for different time periods (days, months, seasons, year) – Figure 4. It is used the conversion from “clear sky” to “real sky” irradiation given in [5].

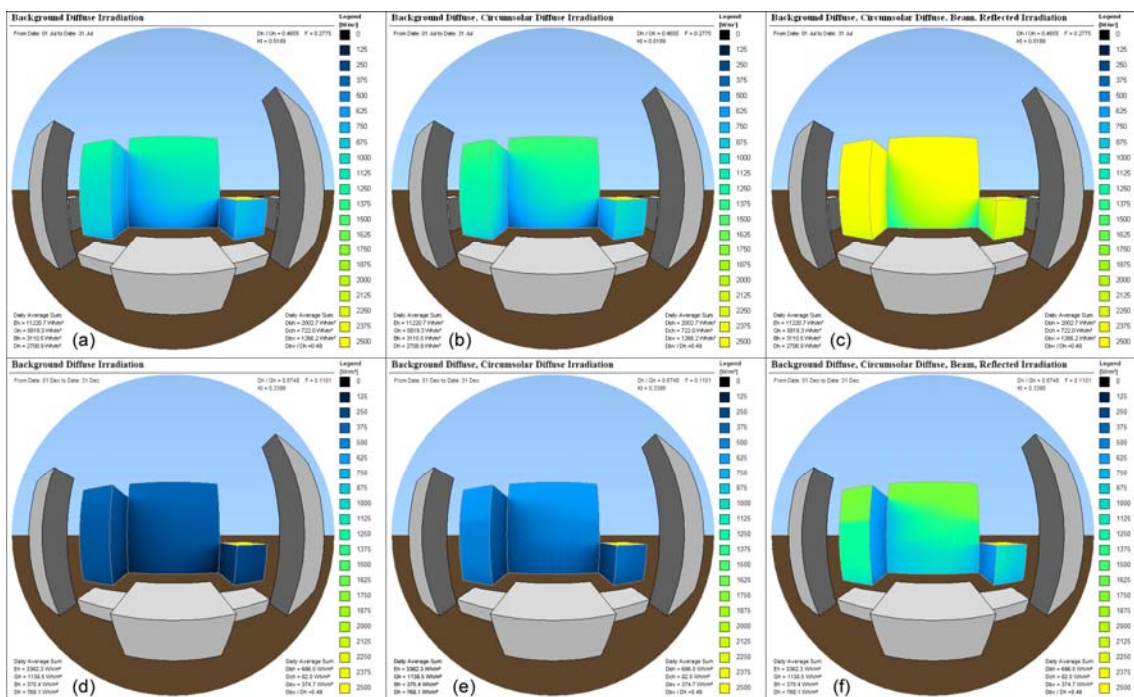


Fig. 4 Exemplary images, generated in 3D–SOLARIA Irradiation Mode – average daily irradiation under a real sky in Sofia: (a) background diffuse irradiation in July; (b) diffuse irradiation in July; (c) diffuse, beam and reflected irradiation in July; (d) background diffuse irradiation in December; (e) diffuse irradiation in December; (f) diffuse, beam and reflected irradiation in December

4 Conclusion

A modified version of the anisotropic irradiance model of Muneer in combination with a new analytical approach to the visible anisotropic sky areas in an urban environment are in the base of new developed program 3D–SOLARIA. Its purpose is to estimate, display and study the variations in the beam and diffuse components of the solar irradiance and solar irradiation for different time periods on the fragments of the building's facades. Even if the modified model needs some additional recalibration, the program could be used to compare the solar potential of the different variants of a future building.

References

- [1] Robinson, D., Haldi, F., Kämpf, J., Leroux, P., Perez, D., Rasheed, A. et al CitySim: Comprehensive micro-simulation of resource flows for sustainable urban planning, *Proceedings of Building Simulation*, Glasgow, 2009, 1083-1090.
- [2] Ivanova, S. M. Estimation of background diffuse irradiance on orthogonal surfaces under partially obstructed anisotropic sky. Part I – Vertical surfaces, *Sol. Energy* (2013), <http://dx.doi.org/10.1016/j.solener.2013.01.021>
- [3] Muneer, T. *Solar radiation and daylight models, second ed.*, Elsevier Butterworth Heinemann, Oxford, 2004
- [4] Photovoltaic Geographical Information System, <http://re.jrc.ec.europa.eu/pvgis/>, 2012.
- [5] Hofierka J., Šúri M. 2002, The solar radiation model for Open source GIS: implementation and applications, *Proceedings of the Open source GIS - GRASS users conference*, Torino, 2002.